



Study of UV Index above Dang, Pokhara and Kathmandu Valley from 2009 to 2020

B. Karki^{1*}, S. H. Dhobi², J. J. Nakarmi³

^{1*}Department of Physics, Trichandra Multiple Campus, Tribhuvan University, Kathmandu-44600, Nepal

^{2,3}Department of Physics, Patan Multiple Campus, Tribhuvan University, Kathmandu-44600, Nepal

²Robotcs Academy of Nepal, Lalitpur-44700, Nepal

²Innovative Ghar Nepal, Lalitpur-44700, Nepal

^{1*}Corresponding Author, Email address: magnum.photon@gmail.com

Received 19 March 2021,
Revised 12 May 2021,
Accepted 14 May 2021

Keywords

- ✓ Dang
- ✓ Pokhara,
- ✓ Kathmandu,
- ✓ UV index,
- ✓ Protection
- ✓ Precaution.

Corresponding Author:
magnum.photon@gmail.com

Abstract

UVI (Ultraviolet Index) levels of considering area from three Valleys: Dang, Pokhara, and Kathmandu for the protection and awareness of the general population, the observed data has been obtained from our research. For our study, we only try to study the UVI numerical value and compare these values to Standard Value categories of UVI provided by or based on WHO guideline. We analyze the UVI on monthly basis and have plotted separately for Dang, Pokhara, and Kathmandu Valley from 2009 to 2020(October). Similarly, we have also analyzed the average UVI for the Comparison of UVI of these three valleys. Upon analysis, it is observed that the UVI above Dang Valley is higher 10+ than that of above Pokhara and Kathmandu Valley, 8+ and 8 respectively, while the minimum above the dang valley is observed to be 4 but above Kathmandu is 3 and Pokhara is 2. Hence, on comparing, researching, and analyzing the people of Pokhara and Kathmandu are less susceptible to exposure to harmful UV than the people of Dang Valley. Also, more precaution, protection, cure, and safety is required for the people of Dang when compared to the other two valleys.

1. Introduction

1.1. Solar Ultra-Violet Radiation

Ultraviolet (UV) radiation falling on the earth's surface originates from the Sun and passes through the atmosphere, where many absorptions and scattering processes occur. The near-UV radiation at wavelengths just shorter than visible light is classified as UV-A (315 to 400 nm). Radiation at progressively shorter wavelengths is more energetic and is classified as UV-B (280 to 315 nm) and UV-C (200 to 280 nm). Atmospheric gases absorb very little UV-A radiation.

Absorption by atmospheric oxygen and ozone prevents all UV-C radiation from reaching the troposphere and the earth's surface. The intensity of UV-B reaching the ground and the short-wavelength cutoff of solar radiation at about 290 nm are strongly influenced by atmospheric ozone. Knowledge of the environment of UV radiation at the earth's surface is important for several reasons. The evolution and growth of most aquatic and terrestrial life forms, including human beings, are influenced by many environmental variables, including the intensity of UV radiation present at the Earth's surface or underwater. In human beings, excessive accumulated exposure can cause skin cancer, eye cataracts, or suppression of the immune system.

Most biological systems respond to UV radiation with effects that generally become more detrimental with decreasing wavelength. The sensitivity of a particular life form to UV radiation is

quantified by an action spectrum such as the erythema skin reddening for human beings, plant damage, and DNA damage. In addition, materials such as plastics are sensitive to exposure to UV radiation, and significant research is being carried out to develop UV resistant materials intended for outdoor use. UV radiation also drives photochemical reactions in the atmosphere and is, therefore, an important consideration for studies of tropospheric pollution [1].

1.2. Measurement of Solar Ultraviolet

Spectral measurements of solar ultraviolet (UV) radiation have been made at several ground-based locations and these measurements are important for two main reasons. First, the measurements combined with results of radiative transfer models contribute toward our understanding of the many complicated radiative transfer processes in the atmosphere and at the Earth's surface. These processes include absorption of radiation by atmospheric gases such as ozone and sulfur dioxide, scattering by atmospheric aerosols and clouds, and scattering from the earth's surface. Knowledge of these processes is required for operational applications such as the estimation of surface UV radiation from satellite data and the forecasting of the UV index. Also, our ability to estimate UV climatology in the past, as well as in the future, requires thorough knowledge of the UV radiative transfer processes.

The second reason for making systematic ground-based measurements of UV radiation is to determine whether long-term changes are occurring as a result of ozone depletion or climate change and to identify specific causes. Examples of how long-term ground-based data records have contributed to our understanding of surface UV radiation are presented. Research on UV radiation includes the measurement of UV radiation at the earth's surface, from airborne platforms including aircraft, balloons, and satellites, or underwater. Ground-based instruments generally measure the intensity of radiation falling on a diffuse horizontal surface. The instruments are usually designed so that the angular response is closely matched to the cosine of the zenith angle of incident radiation.

Long-term data records can be used to detect long-term changes in UV-B radiation that may be attributed to changes in atmospheric ozone. Combining the UV measurements with those of other variables such as total ozone, cloud cover, aerosol optical depth, surface albedo, or reflectivity from space-based satellite data enables the development of statistical relationships that establish the dependence of UV on absorption and scattering processes. Three main types of instruments are used for measuring UV radiation: spectral, broadband, and multifilter narrowband.

1.3. Importance of Solar Ultraviolet

Solar Spectrum Solar radiation is of paramount importance for nearly all studies regarding the earth's geophysical properties and biological behaviour. The solar spectrum is used as input for radiative transfer, dynamical, and photochemical models that simulate the real atmosphere. The absolute intensity of surface UV irradiance at a given wavelength is proportional to the radiative output from the Sun at the same wavelength [2].

Therefore, spectral features of the solar spectrum are present in surface UV irradiance, which compares space-based measurements of the solar spectrum with ground-based measurements of surface UV irradiance. Radiation below 300 nm is important for driving many atmospheric photochemical processes [3]. More recently, space-based measurements from satellite instruments have measured the absolute intensity of the solar spectrum. Comparison of the solar spectrum measured from different satellite instruments agree to within 63%, a value that is similar to results of comparisons between direct space-based measurements and ground-based Langley plot measurements [4].

1.4. Effect of Ultraviolet Radiation on earth

A major goal for researching UV radiation is to determine accurately the wavelength dependence and angular dependence of UV at the earth's surface and underwater continuously and on a global scale. Measuring the UV environment everywhere all the time at a resolution pertinent to local biological systems is an impossible task. Advances toward this goal can only be achieved with a thorough understanding of the factors that affect surface UV radiation.

The quantity and quality of ground-based spectral irradiance measurements have increased significantly over the last 10 yr. Comparisons of satellite retrievals and radiative transfer computer models with the ground-based data have uncovered problems with the measurements, the interpretation of the data, and the models. Currently, important applications of our understanding include

- The routine daily forecasting of the UV index [5].
- Global or regional estimates of surface UV irradiance using satellite irradiance and reflectivity data [6].
- Global estimates of the penetration of UV irradiance into natural waters [7].
- The extension of spectral UV irradiance estimates in space using ancillary data. These measurements have been used to determine surface UV irradiance values averaged over several years for large areas of land.
- The extension of spectral surface UV irradiance records into the past using satellite data records. Satellite estimates indicate that surface UV increased from mid to high latitudes between 1979 and 1992.
- The extension of spectral surface UV irradiance back to the 1960s using ground-based total ozone data with pyranometer global radiation measurements, humidity, and snow cover information.

These results indicate that there have been decadal increases in surface UV irradiance, but the changes are due to causes other than ozone at some sites. Comparisons of satellite retrievals with ground-based measurements indicate that the satellite data is generally between 0 and 40% higher than the ground-based measurements, [8] with better agreement at cleaner sites.

1.5. Factor Affecting UV

The ultraviolet (UV) band of the electromagnetic spectrum extends from 100 to 400 nm and is divided into three sub-regions: the UV-C, UV-B and UV-A. Only a small fraction (9.3%) of the electromagnetic radiation emitted by the Sun is in the UV spectral region as most of it is attenuated by the Earth's atmosphere as it propagates toward the surface. Despite the small amount of UV radiation that finally reaches the Earth's surface, its biological significance is exceptional [9]. UV radiation triggers and/or drives photochemical and photobiological processes, which are necessary for the proper functioning of ecosystems, and has strong direct or indirect effects on human health. Living organisms have slowly adapted to the current levels of solar UV radiation through the evolution process and fast or abrupt changes impact the health and the diversity of flora and fauna [10]. Consequently, any change in the ecosystems affects human populations through their interaction with the natural environment. UV radiation that reaches the surface of the Earth exhibits periodical changes associated with several different phenomena: the solar radiation that reaches the Earth's atmosphere changes by $\pm 3\%$ in the year as a result of periodical changes in the Earth-Sun distance while the angle between the Sun and the zenith of a particular place on Earth also changes periodically leading to corresponding changes in the radiant energy. Periodical changes in solar activity, such as the 11-year solar cycle, the 27-day apparent solar rotation, and dynamical atmospheric processes also induce changes in the levels of solar UV radiation that reach the Earth's surface.

Living organisms have adapted to the above periodicities, which are predictable and easily modelled. Non-periodic changes in atmospheric composition and dynamics can also affect the levels of surface UV radiation significantly. Solar UV radiation at wavelengths below 290 nm is absorbed by molecular oxygen and the ozone at the higher atmosphere and does not enter the troposphere. Atmospheric molecules scatter radiation more effectively with decreasing wavelength, thus scatter more UV than visible or infrared light. The ozone effectively absorbs UV-B radiation, allowing only a very small fraction to reach the Earth's surface. In addition to the ozone, other gases also absorb part of the UV radiation (e.g., SO₂ and NO₂), though their impact is usually less significant than that of the ozone, either because their absorption efficiency is smaller or because they are less abundant than the ozone. Clouds and aerosols in the troposphere also scatter (both clouds and aerosols) and absorb (aerosols) solar UV radiation. The spectral attenuation by clouds and aerosols depends on their type and characteristics [11]. Clouds are the most significant driver of the short-term variability of UV irradiance at the Earth's surface. Although they usually attenuate UV radiation, under particular conditions UV irradiance can be enhanced due to the presence of clouds. In urban environments changes in aerosols may counterbalance the effect of even extremely high or low total ozone events, and lead to erythemal irradiance above or below the climatological averages respectively [12].

1.6. Solar UV Index

The UV index has been calculated using the effective spectrum for erythema described in Webb et al. (2011). Averages of the irradiance in the range 305–310 nm (from now on referred to as 307.5 nm irradiance) and 320–325 nm (hereafter referred to as 322.5 nm irradiance) have been calculated and analyzed instead of measurements at the central wavelengths of the two bands. This way the effects of the technical characteristics of each instrument are minimized and the comparison between the irradiance at the two stations is more reliable. Increased surface albedo enhances the irradiance in the UV-B more effectively than in the UV-A region, while the spectral effects of clouds and aerosols vary depending on their characteristics. However, the spectral effect of clouds, aerosols, and surface albedo is usually insignificant relative to the spectral effect of ozone, which has a much stronger effect on the 307.5 nm relative to the 322.5 nm irradiance [13]. To describe the levels of UV irradiance that reaches the earth's surface more comprehensively, a simple index was adopted. The higher the UVI values; the greater the risk of sunburn, thus protective measures should be taken. Apart from the knowledge of the UVI that can be obtained from several online tools and/or cell phones applications as a prognostic parameter; the skin type should also be identified [14].

2. Review

Long-term trends of UV irradiance, and their main drivers, vary significantly throughout Europe. Analysis of total ozone and spectral UV data recorded at four European stations during 1996–2017 reveals that long-term changes in UV are mainly driven by changes in aerosols, cloudiness, and surface albedo, while changes in total ozone play a less significant role. The variability of UV irradiance is large throughout Italy due to the complex topography and large latitudinal extension of the country. Analysis of the spectral UV records of the urban site of Rome, and the alpine site of Aosta reveals that differences between the two sites follow the annual cycle of the differences in cloudiness and surface albedo. Comparisons between the noon UV index measured at the ground at the same stations and the corresponding estimates from the Deutscher Wetterdienst (DWD) forecast model and the ozone monitoring instrument (OMI)/Aura observations reveal differences of up to 6 units between individual measurements, which are likely due to the different spatial resolution of the different datasets, and

average differences of 0.5–1 unit, possibly related to the use of climatological surface albedo and aerosol optical properties in the retrieval algorithms [15].

Long term decline in column ozone over northern mid-latitudes is about 2% in summer and 4% in winter-spring, yielding a 2.5% and 5% increase in UV Index respectively. Long-term changes in cloud cover can also affect UV Index values. Analyses of reconstructed data sets over central and eastern Europe since the 1960s indicate a ~10% change in UV Index due to variations in cloud cover. Local trends in absorbing aerosols can also have a noticeable effect on the UV Index. For example, a more than 10% increase in UV-B in Thessaloniki, Greece, is likely due to a decrease in aerosols.

Long-term fluctuations in mean daily erythemal UV doses for Toronto calculated from actual spectral UV measurements and reconstructed from global solar radiation and ozone. The somewhat elevated UV level in the 1990s and 2000s is related to the ozone decline, and the large year-to-year fluctuations are caused by natural fluctuations in cloud cover and ozone. Forecasts and public awareness program Environment Canada issues the UV Index in its weather forecasts to increase awareness of the harmful effects of UV radiation, support the education of the public on UV risks and encourage people to take action for protection.

Comparisons of forecasted UV Index values with measurements show that the overall agreement between predicted and observed values is about ± 1.4 Index units. Dividing the comparison into various weather conditions indicates that agreement is best under sunny or mainly sunny conditions (± 0.7 units). In general, the agreement degrades (>1.5 units) under other conditions, such as partial clouds, overcast skies or precipitation. Environment Canada introduced a renewed UV Index program in February 2004 based on the recommendations contained in the World Health Organization's Global Solar UV Index Practical Guide of 2002.

The UV Index is categorized into low (less than 2), moderate (3 to 5), high (6 and 7), very high (8 to 10) and extreme (11 and above). Media coverage of the UV Index varies considerably by region. It is available from Environment Canada in the public weather forecasts whenever the maximum value is expected to reach 3 or higher [16]. The clear sky UV-index is expressed as a function of two predictable quantities: the solar zenith angle and total ozone. This new function gives good results for all solar zenith angles between 0° and 90° and a wide range of total ozone values. An unbroken cloud layer typically reduces the UVI by 50 to 60% and even more during precipitation. A broken cloud layer can increase or decrease the UVI.

The ultraviolet albedo is quite low for most surfaces, and so the influence of the albedo on the UVI is minimal. A UVB increase of 28% over a snow cover under clear sky conditions has been reported by McKenzie et al. (1998). The distribution of ozone through the atmosphere has a remarkably strong influence on UVI. Model simulations show that the calculated UVI values increase by 8% when a mid-latitude ozone profile is replaced by a tropical profile while keeping the total amount of ozone constant. An enhanced ozone content in the boundary layer ('smog') will result in lower UVI values. A model study shows a decrease of about 3%.

The average optical depth is 0.346 ± 0.210 , with a typical Angstrom parameter of 1.4. Ignoring the variations in aerosol by assuming typical values for the aerosol optical depth introduces an error of about 5% in the UVI. In the absence of snow, UVI will increase some 5% per kilometre altitude for high plateaus due to a decrease in Rayleigh scattering. In mid-latitudes, the total ozone distribution shows a substantial day-to-day variability. The distance between the Earth and the Sun is not constant. The solar irradiance deviates by $\pm 3\%$ around its mean value, with a maximum in January. The ozone absorption coefficients are slightly temperature-dependent. However, the stratospheric temperature can

vary significantly, especially in the vicinity of the polar vortex. The effects of other minor trace gases are of comparable magnitude [17, 18, 19].

The air pollutant is found for Lumbini is 18 minimum to 209 maximum, for Dang is 26 minimum to 119 maximum, for Chitwan is 42 minimum to 176 maximum, for Nepalgunj 21 minimum to 178, and Shurkhate 73 minimum to 119 maximum. The air quality present between 2016 to now 2020 is not quite bad but unhealthy and moderate. These air size help to increasing the atmospheric temperature after collision with aircraft [20, 21]. The pollution of these valley increasing day by days [22, 23]. The UVs rays energy kill the virus and bacteria because of high energy therefore in this cases UVs has beneficial to human [24]. Moreover, the energy of UVs light ranges from 3.10 to 12.4eV and the bond energy of carbon and oxygen in free carbon dioxide is 2.94eV. Therefore it may help to produce the oxygen from carbon dioxide [25, 26].

3. Methodology

Erythemally Effective UV promotes a standardized public health measure for reporting the UV irradiance by WHO. The internationally adopted UVI standard erythema reaction in human skin. The relative effectiveness of wavelengths responsible for any biological reaction including an erythema reaction is collectively known as Action Spectra includes several categories or bands on an open-ended linear scale. The UVI weights the spectral surface irradiance to those wavelengths that cause a sun burning [27, 28].

Table 1. UV index Categories [29, 30, 31].

Category	Color Code	UVI	$E_{ery}(mW/m^2)$
Low	Green	0-2	0-75
Moderate	Yellow	3-5	75-150
High	Orange	6-7	150-200
Very High	Red	8-10	200-275
Extreme	Purple	11+	275+

The activities introduce and build an understanding of integral calculus and trigonometric functions through the presentation of practical problem solving that focuses on Public Health and developing a personal understanding of solar ultraviolet radiation and the UV Index. These activities also develop critical thinking skills through the application of data mining, data processing and presentation. They also emphasize the importance of drawing valid conclusions, concepts important to scientific research, statistics and epidemiology. Total irradiance could be estimated as a Riemann sum where the UV irradiance, E_{total} (W/m^2) is determined by integrating the spectral irradiance concerning wavelength as:

$$E_{total} = \int_{\lambda=290nm}^{400nm} E(\lambda)d\lambda \quad Eqn. 1$$

Moreover, Eqn.1 can be written in summation form with the product of Spectral Irradiance $E(\lambda)$ and wavelength $d\lambda$ as

$$E_{total} \approx \sum_{\lambda=290nm}^{400nm} E(\lambda)d\lambda \quad Eqn. 2$$

This numerical approximation accurately measures the integrated spectral UV surface irradiance provided $d\lambda$ is small [32]. The erythemally effective UV irradiance, E_{ery} at 12:00 P.M becomes $0.155 W/m^2$ (and only $0.022 W/m^2$ at 8:00 am). This is measured by weighting the incident spectral UV irradiance with the erythemally effective action spectrum, $A(\lambda)$ and determining the integral numerically.

$$E_{ery} = \sum_{\lambda=290nm}^{400nm} A(\lambda)E(\lambda)d\lambda \quad Eqn. 3$$

The UVI is typically employed to represent the meaning of these low magnitude integrals of erythemally weighted solar radiation at the Earth's surface. As an index, the UVI has no units and is formally defined by the ratio,

$$UVI = \frac{E_{ery}}{25} \quad Eqn. 4$$

where E_{ery} is expressed in mW. Note that a UVI of 1 corresponds to 25 mW/m² of erythemally effective solar radiation, the same amount of energy used per second by a typical LED. Similarly, a UVI of 10 represents 250 mW/m² of erythemally effective radiation.

3.1. Research area

Dang Valley: It is located in Inner Terai in Lumbini Province in midwestern Nepal. The district with a population of 548,141 (2011) has Ghorahi as its headquarters and covers 2,955 km². Tulsipur, the second biggest city in Dang, is a transportation hub.

Pokhara Valley: Pokhara Valley, located in the Gandaki zone is the second-largest valley in the hilly region. It is 203 kilometres (126 mi) west of Kathmandu Valley. The current metro area population of Pokhara in 2020 is 421,000, a 4.73% increase from 2019.

Kathmandu Valley: The Kathmandu valley includes 3 cities – Kathmandu, Lalitpur and Bhaktapur with a total area of 570 sq. km. The population of the valley is 2.5 million with an annual growth rate of 4.63% (3.5 million unofficial). This represents 9.32% of the entire population of the country.

3.2. Data Analysis

The Comparative study of UVI of Dang, Pokhara, and Kathmandu Valley 2009-2020 data was obtained from www.worldweatheronline.com. The statistical analysis is performed to illustrate the monthly changes in UV radiation. [Table 2](#) below is an average UVI of every month from 2009-2020.

Table 2: Average UVI above Dang, Pokhara, and Kathmandu Valley 2009-2020 [33]

Month	Average UV Index above Kathmandu	Average UV Index above Dang	Average UV Index above Pokhara
January	3.083	4.83	2.92
February	3.833	5.75	3.25
March	4.75	7.33	4.17
April	5.33	8.25	4.92
May	5.33	8.42	5.08
June	5.08	8	5.17
July	5	7.33	4.75
August	5.12	6.91	5
September	4.92	7	4.92
October	4.08	6.17	4
November	3.73	5.36	2.91
December	3.09	4.64	2.55

4. Result and Discussion

4.1. UV Index above Kathmandu Valley from 2009 to 2020

The observed data is based on the maximum UVI with corresponding months and the plot show monthly maximum UVI variation through the year 2009 to 2020 (October). On studying the observation shown

in 2020 the maximum UVI is 7 in March, in 2009 it is 6 in April; in 2010 it is 6 in April, May, June and August; in 2011 it is 5 in April, May, August and September; in 2012 it is 6 in May, June, and July; in 2013 it is 6 in July; in 2014 it is 6 in April, May, July August; in 2015 it is 6 in April, May and June; in 2016 it is 5 in July August and September; in 2017 it is 5 from April to September; in 2018 it is 5 in April, May, August and September; in 2019 it is 6 from April to June, and in 2020 the maximum value is 7 in March (Figure 1).

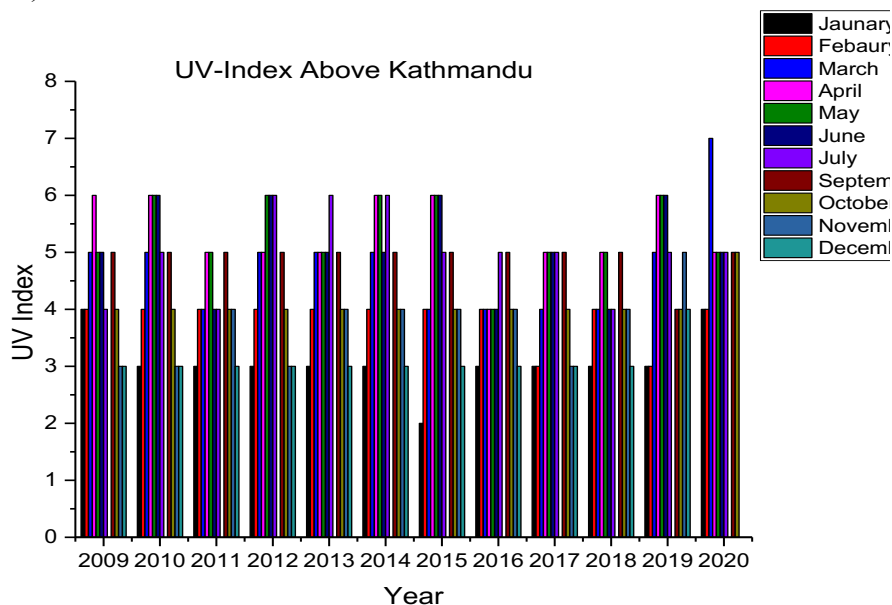


Figure 1: Bar graph for the representation UVI of Kathmandu Valley

Table 3: Minimum and Maximum UVI of Kathmandu Valley

Year	Maximum	Minimum
2009	6	3
2010	6	3
2011	5	3
2012	6	3
2013	6	3
2014	6	3
2015	6	3
2016	5	3
2017	5	3
2018	5	3
2019	6	3
2020	7	3

4.2. UV Index above Pokhara Valley from 2009 to 2020

The observed data is based on the maximum UVI with corresponding months and the plot show monthly maximum UVI variation through the year 2009 to 2020 (October). On studying the observation shown in 2019 the maximum UVI is 8 in April, in 2009 it is 6 in April; in 2010 it is 6 in June; in 2011 it is 5 in May, August and September; in 2012 it is 6 in May and June; in 2013 it is 5 in April, June, July, August and September; in 2014 it is 6 in June; in 2015 it is 5 in June, August and September; in 2016 it is 5 in April and September; in 2017 it is 5 in May, July, August, and September; in 2018 it is 5 in May, June, August and September; in 2020 it is 7 in October (Figure 2).

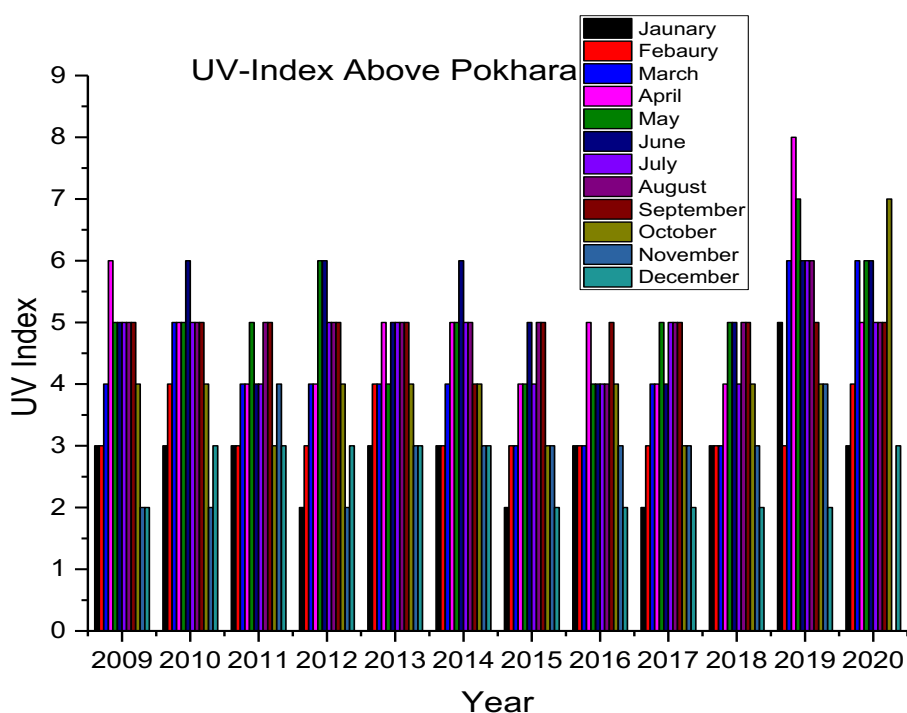


Figure 2: Bar graph for the representation UVI of Pokhara Valley

Table 4: Minimum and Maximum UVI of Pokhara Valley

Year	Maximum	Minimum
2009	6	2
2010	6	2
2011	5	3
2012	6	2
2013	5	3
2014	6	3
2015	5	2
2016	5	2
2017	5	2
2018	5	2
2019	8	3
2020	7	3

4.3. UV Index above Dang Valley 2009 to 2020

The observed data is based on the maximum UVI with the corresponding months and the plot show monthly maximum UVI variation through the year 2009 to 2020 (October). On studying the observation shown in 2019 the maximum UVI is 10 in May, in 2009 it is 9 in April and June; in 2010 it is 9 in May and June; in 2011 it is 8 in April; in 2012 it is 9 in May and June; in 2013 it is 9 in April; in 2014 it is 9 in May and June; in 2015 it is 9 in May; in 2016 it is 8 in April, May, and June; in 2017 it is 8 in March to July; in 2018 it is 8 in April and May; in 2020 the maximum UVI observed is 8 in May (Figure 3, Table 5).

4.4. Average UV Index above Kathmandu, Pokhara and Dang Valley from 2009 to 2020

The comparison of combined average data of UVI monthly from 2009 to 2020 are shown below and observed that Dang valley have high UVI in comparison to Kathmandu and Pokhara Valley. It is also observed that the minimum UVI is 2 in January and December above Pokhara while maximum 8+ in May above Dang (Figure 4).

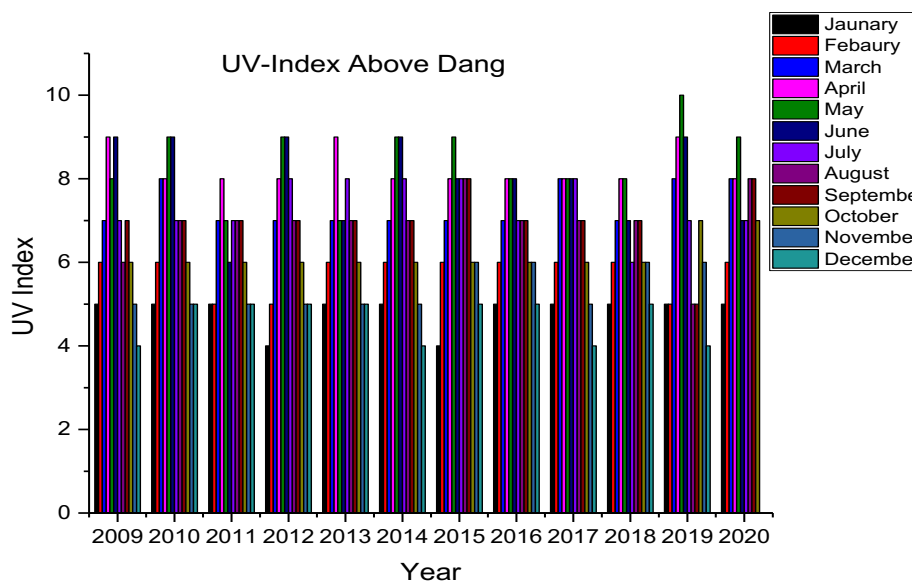


Figure 3: Bar graph for the representation UVI of Dang Valley

Table 5: Minimum and Maximum UVI of Dang Valley

Year	Maximum	Minimum
2009	9	4
2010	9	5
2011	8	5
2012	9	5
2013	9	5
2014	9	5
2015	9	4
2016	8	5
2017	8	4
2018	8	5
2019	10	4
2020	9	5

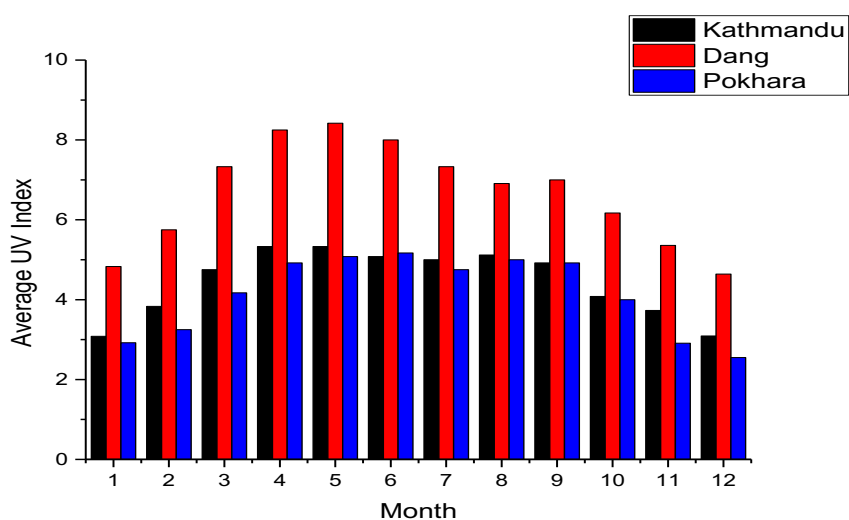


Figure 4: Average UVI above Dang, Kathmandu, and Pokhara Valley

4.5. Standard Deviation of collection data

The standard deviation of the data above Dang, Pokhara and Kathmandu are listed in Table 6 below:

Table 6: SD of Pokhara Kathmandu and Dang Valley

Month	Pokhara SD	Kathmandu SD	Dang SD
January	0.79	0.51	0.39
February	0.45	0.39	0.45
March	1.03	0.87	0.49
April	1.16	0.65	0.45
May	0.9	0.65	0.9
June	0.83	0.79	1.04
July	0.62	0.74	0.65
August	0.43	0.38	0.79
September	0.29	0.29	0.74
October	1.04	0.29	0.39
November	0.7	0.65	0.5
December	0.52	0.3	0.55

5. Conclusion

By observing the data for UVI above Dang, Pokhara and Kathmandu Valley, it is seen that the UVI above Dang is higher than that of Kathmandu and Pokhara. The maximum UVI observed above Dang is up to 10+ which belongs to Extreme Categories and Minimum 4 which belongs to Moderate categories with comparison to the standard value mention by WHO. While the maximum UVI observed above Pokhara and Kathmandu are up to 8 and 7, and the minimum is 2 and 3 respectively. For the maximum value of UVI above Pokhara and Kathmandu belong to high and very high categories but minimum belong to moderate and Low categories.

Therefore, throughout the year the population of dang valley needed protection from UV Radiation while for the people of Kathmandu and Pokhara it was only for certain months.

Conflict of Interest: The authors declare that there are no conflicts of interest.

Authors Contribution: Equally Contribute

Compliance with Ethical Standards: This article does not contain any studies involving human or animal subjects.

Acknowledgement

We would like to thanks all the members of the Department of Physics, Tri-Chandra Multiple Campus, Kathmandu-44600, Tribhuvan University and Department of physics, Patan Multiple Campus, Lalitpur-44700, Robotic Academy of Nepal, Innovative Ghar Nepal, Lalitpur-44700, and National Research Council Nepal for their kind support during this work.

Reference

- [1] J. B. Kerr, Understanding the factors that affect surface ultraviolet radiation, *Optical Engineering*, 44, 4 (2005) 1-2.
- [2] A. Berk, G. P. Anderson, P. K. Acharya, J. H. Chetwynd, L. S. Bernstein, E. P. Shettle, M. W. Matthew, and S. M. Adler-Golden, *Modtran User's Manual*, Air Force Research Laboratory, Hamscon AFB, MA (1999).
- [3] H. Neckel, and D. Labs, The solar radiation between 3300 Å and 12500 Å, *Solar Physics*, 90 (1984) 205–258. <https://doi.org/10.1007/BF00173953>

- [4] A. F. Bais, Absolute spectral measurements of direct solar ultraviolet irradiance with a Brewer spectrophotometer, *Applied Optics*, 36,21 (1997) 5199– 5204.
<https://doi.org/10.1364/AO.36.005199>
- [5] W. R. Burrows, M. Vallee, D. I. Wardle, J. B. Kerr, L. J. Wilson, and D. W. Tarasick, The Canadian operational procedure for forecasting total ozone and UV radiation, *Meteorology Applied*, 1,3 (1994) 247–265.
- [6] T. F. Eck, P. K. Bhartia, and J. B. Kerr, Satellite estimation of spectral UV-B irradiance using TOMS derived ozone and reflectivity, *Geophysics Research Letter*, 22 (1995) 611–614.
<https://doi.org/10.1029/95GL00111>
- [7] A. P. Vasilkov, J. Herman, N. A. Krotkov, M. Kahru, B. G. Mitchell, and C. Hsu, Problems in the assessment of the ultraviolet penetration into natural waters from space-based measurements, *Optical Engineering*, 41, 12 (2002) 3019–3027.
- [8] R. L. McKenzie, G. Seckmeyer, A. F. Bais, J. B. Kerr, and S. Madronich, Satellite retrievals of erythemal UV dose compared with ground-based measurements at northern and southern midlatitudes, *Journal Geophysics Research*, 106 (2001) 24051–24062.
<https://doi.org/10.1029/2001JD000545>
- [9] K.N. Liou, *An Introduction to Atmospheric Radiation*, Elsevier Science: Amsterdam, The Netherlands, (2002).
- [10] J.F. Bornman, P.W. Barnes, T.M. Robson, S.A. Robinson, M.A.K. Jansen, C.L. Ballaré, S.D. Flint, Linkages between stratospheric ozone, UV radiation and climate change and their implications for terrestrial ecosystems, *Photochemical and Photobiology Science*, 18 (2019) 681–716.
<https://doi.org/10.1039/C8PP90061B>
- [11] A.F. Bais, C.S. Zerefos, C. Meleti, I.C. Ziomas, and K. Tourpali, Spectral measurements of solar UVB radiation and its relations to total ozone, SO₂, and clouds, *Journal of Geophysics Research Atmosphere*, 98, D3 (1993) 5199–5204. <https://doi.org/10.1029/92JD02904>
- [12] G. Seckmeyer, D. Pissulla, M. Glandorf, D. Henriques, B. Johnsen, A. Webb, A.M. Siani, A. Bais, B. Kjeldstad, and C. Brogniez et al., Variability of UV Irradiance in Europe, *Photochemical Photobiology*, 84, 1 (2008) 172–179. <https://doi.org/10.1111/j.1751-1097.2007.00216.x>
- [13] R.L. McKenzie, C. Weinreis, P.V. Johnston, B. Liley, H. Shiona, M. Kotkamp, D. Smale, N. Takegawa, and Y. Kondo, Effects of urban pollution on UV spectral irradiances, *Atmosphere Chemical Physics*, 8, 18 (2008) 5683–5697. <https://doi.org/10.5194/acp-8-5683-2008>
- [14] <https://uvb.nrel.colostate.edu/UVB/publications/UV-Primer.pdf> assessed in August 2020.
- [15] I. Fountoulakis, H. Diémoz, A.M. Siani, G. Laschewski, G. Filippa, A. Arola, A. F. Bais, H. D. Backer, K. Lakkala, A. R. Webb, V.D. Bock, T. Karppinen, K. Garage, J. Kapsomenakis, M. E. Koukouli, and C. S. Zerefos, Solar UV Irradiance in a Changing Climate: Trends in Europe and the Significance of Spectral Monitoring in Italy, *Environments*, 7,1 (2020) 1-2.
[doi10.3390/environments7010001](https://doi.org/10.3390/environments7010001)
- [16] V. Fioletov, J.B. Kerr, and A. Fergusson, The UV Index: Definition, Distribution and Factors Affecting It, *Canadian Journal of Public Health*, 101,4 (2010) 15-19.
<http://dx.doi.org/10.1016/j.atmosres.2012.01.005>
- [17] M. Allaart, M.V. Weele, P. Fortuin, and H. Kelder, An empirical model to predict the UV-index based on solar zenith angles and total ozone, *Meteorological Applications*, 11,1 (2004) 59–65.
<https://doi.org/10.1017/S1350482703001130>
- [18] W.M.F. Wauben, and F. Kuik, A Sensitivity study of the Brewer direct sun ozone retrieval algorithm using numerical simulations, *Proc. XVIII Quadr. Ozone Symp., Aquila*, 85– 88, (1998).

- [19] H. J. Eskes, P. F. J. Velthoven, P. J. M. Valks, and H. M. Kelder, Global ozone forecasting based on ERS-2 GOME observations, *Atmosphere Chemistry Physics*, 2 (2002) 271–278. <https://hal.archives-ouvertes.fr/hal-00295205>
- [20] S. H. Dhobi, Comparative Study of Air Quality of West Terai, Nepal, *International Journal of Multidisciplinary Sciences and Advanced Technology*, 1,8 (2020) 1-9. doi:10.9790/2402-1405022935.
- [21] S. H. Dhobi, A. Panthi, S. Panthi, and R. Subedi, Development of Mathematical Model to Study the Variation Temperature due to the Collision of Air Molecules or Aerosol Particle with Aircraft, *European Journal of Applied Physics*, 3, 3 (2021) 1-5. <http://dx.doi.org/10.24018/ejphysics.2021.3.3.70>
- [22] S. Gautam, S. H. Dhobi, Study and Analysis of Pb Acid and Li-Ion Battery for Transport, Safa Tempo in Kathmandu Valley, *International Journal of Engineering and Artificial Intelligence*, 2,2 (2021) 53–59.
- [23] S. G. Tamang, R. C. Pagani, S. H. Dhobi, Problem Faced by Classical Electrical Vehicles and Solution in Kathmandu, *International Journal of education and applied research*, 9,1 (2019) 20-24.
- [24] S. H. Dhobi, S. Karki, B. Karki, B. Shrestha, A. Karki, R. Basnet, Killing Coronavirus Before They Enter Human Body, *International Journal of Multidisciplinary Sciences and Advanced Technology*, 1, Sp. 2, (2020) 90–96.
- [25] S. H. Dhobi, A Model to Convert CO₂ into O₂ with Photons, *International Journal of Multidisciplinary Sciences and Advanced Technology*, 1,4 (2020) 13–21.
- [26] S. H. Dhobi, B. Karki, Removal Of Global Warming Using CBGT Device, *International Journal of Advanced Research and Publications*, 1,5, 189-192, (2017).
- [27] <http://www.who.int/uv/publications/en/UVIGuide.pdf> assessed at September 2020
- [28] World Meteorological Organization, Report of the WMO-WHO meeting of experts on standardization of UV indices and their dissemination to the public, (Report 127), Switzerland, (1997).
- [29] CIE (International Commission on Illumination), Research Note 1986, 19-23 (1986).
- [30] CIE (International Commission on Illumination), Erythema reference action spectrum and standard erythema dose, CIE S007E-1998 Vienna: CIE Central Bureau, (1998).
- [31] CIE (International Commission on Illumination) Action spectrum for the production of previtamin D3 in human skin, Note 174, (2006).
- [32] N. Downs, A.V. Parisi, L. Galligan, J. Turner, A. Amar, R. King, F. Ultra, and H. Butler, Solar radiation and the UV index: An application of numerical integration, trigonometric functions, online education and the modelling process, *International Journal of Research in Education and Science*, 2,1 (2016) 179-189.
- [33] <https://www.worldweatheronline.com> assessed in October 2020.

(2021) ; <http://www.jmaterenvirosci.com>